In Vivo Predictive Dissolution: Comparing the Effect of Bicarbonate and Phosphate Buffer on the Dissolution of Weak Acids and Weak Bases

BRIAN J. KRIEG,[1] SEYED MOHAMMAD TAGHAVI,[2] GORDON L. AMIDON,[1] GREGORY E. AMIDON[1]

[1]College of Pharmacy, University of Michigan, Ann Arbor Michigan 48109
[2]Department of Chemical Engineering, Laval University, Quebec, Quebec City G1V 0A6, Canada

Received 30 October 2014; revised 29 March 2015; accepted 1 April 2015

Published online 15 May 2015 in Wiley Online Library (wileyonlinelibrary.com). DOI 10.1002/jps.24460

ABSTRACT: Bicarbonate is the main buffer in the small intestine and it is well known that buffer properties such as pK_a can affect the dissolution rate of ionizable drugs. However, bicarbonate buffer is complicated to work with experimentally. Finding a suitable substitute for bicarbonate buffer may provide a way to perform more physiologically relevant dissolution tests. The dissolution of weak acid and weak base drugs was conducted in bicarbonate and phosphate buffer using rotating disk dissolution methodology. Experimental results were compared with the predicted results using the film model approach of (Mooney K, Mintun M, Himmelstein K, Stella V. 1981. J Pharm Sci 70(1):22–32) based on equilibrium assumptions as well as a model accounting for the slow hydration reaction, $CO_2 + H_2O \rightarrow H_2CO_3$. Assuming carbonic acid is irreversible in the dehydration direction: $CO_2 + H_2O \leftarrow H_2CO_3$, the transport analysis can accurately predict rotating disk dissolution of weak acid and weak base drugs in bicarbonate buffer. The predictions show that matching the dissolution of weak acid and weak base drugs in phosphate and bicarbonate buffer is possible. The phosphate buffer concentration necessary to match physiologically relevant bicarbonate buffer [e.g., 10.5 mM (HCO_3^-), pH = 6.5] is typically in the range of 1–25 mM and is very dependent upon drug solubility and pK_a. © 2015 Wiley Periodicals, Inc. and the American Pharmacists Association J Pharm Sci 104:2894–2904, 2015

Keywords: Dissolution; mathematical model; gastrointestinal; diffusion; physicochemical properties; transport; in vitro models; acid-base equilibria

INTRODUCTION

Dissolution can be an important diagnostic tool for predicting the *in vivo* effects when a drug product is administered orally. The identification of an *in vitro* dissolution test that accurately predicts *in vivo* dissolution is therefore essential. Bicarbonate (HCO_3^-) is secreted by the pancreas and epithelial cells in the small intestine to neutralize gastric acid emptied into the duodenum and buffer the intestinal fluid maintaining intestinal pH. Conducting dissolution experiments in bicarbonate buffer would be more physiologically realistic. However, the preparation of physiologically relevant bicarbonate buffer is complex experimentally. CO_2 gas must be constantly added to water to obtain a constant bicarbonate buffer concentration. This is generally a slow process that can also affect the hydrodynamics and dissolution of drug product/particles because of the potential presence of gas bubbles at solid–liquid interfaces. Therefore, using a buffer solution that produces equivalent buffer effect on drug dissolution as bicarbonate buffer would be preferred.

Phosphate buffer is a logical buffer to consider to match the effect of bicarbonate buffer on dissolution. It is commonly used in dissolution testing and is a buffer proposed by US FDA to be used for *in vivo* biowaivers.[1] The relevant pK_a of phosphate (6.8) is within the pH range of the small intestine and therefore makes it a suitable buffer to be considered for physiologically relevant dissolution tests. Additionally, the dissolution of weak acid drugs has been accurately predicted in phosphate buffer using the film model and reaction plane model.[2–4] Therefore, there is already precedence for making accurate predictions of dissolution in phosphate buffer that is further supported in this paper. This work provides greater insight by using a wide range of phosphate buffer concentrations to match dissolution in bicarbonate buffer.

Phosphate buffer is currently used today as the buffer component in USP simulated intestinal fluid at pH 6.8, and in fasted-state simulated intestinal fluid at pH 6.5 with concentrations/buffer capacities of 50 mM/29 mM/ΔpH and 29 mM/15 mM/ΔpH, respectively.[5,6] In comparison, the average bicarbonate buffer concentrations in the small intestine are approximately 6–20 mM that correspond to a buffer capacity range of 2.5–8.5 mM/ΔpH at a pH of 6.5.[7] This calculated buffer capacity corresponds very well with reported data for measured buffer capacities in human intestinal fluid that are within this same range of 2.48–13 mM/ΔpH.[8–12] The difference in physiological bicarbonate buffer concentration/capacity compared with typical phosphate buffer concentration/capacity highlights the difference between the dissolution media that is currently used compared with the fluid present in the small intestine. These differences have been studied experimentally and significant differences in dissolution between physiologically relevant bicarbonate buffer and phosphate buffer have been observed.[4,13–16] However, the differences observed in the dissolution rates are not only caused by the different buffer concentration/capacity used in the dissolution experiments. The physicochemical properties of the drug will impact the pH at the surface of the dissolving drug that makes matching dissolution rates in two different buffer systems more complex than matching buffer capacities in the bulk solution. The

Correspondence to: Gregory E. Amidon (Telephone: +419-410-1575; Fax: +734-615-6162; E-mail: geamidon@umich.edu)

Journal of Pharmaceutical Sciences, Vol. 104, 2894–2904 (2015)

physicochemical properties of the drug and buffer must be taken into account to accurately predict how a drug will dissolve in each buffer system.

Krieg et al.[17] have demonstrated the importance of reaction kinetics on the ability of bicarbonate to buffer the bulk aqueous pH as well as the pH at the surface of the dissolving drug. These reaction rate considerations introduce an additional complexity for matching the buffer capacities of bicarbonate and phosphate.

In the bulk aqueous phase where equilibrium conditions may be assumed, the buffer capacity of the CO_2–bicarbonate buffer behaves according to Reaction (1) with a buffer pK_a of 6.04 (Bulk Chemical Equilibrium model: BCE model). This equilibrium is achieved in the bulk solution because the chemical reactions have an extended period of time to take place.

$$CO_2\,(aq) + H_2O \rightleftharpoons H_2CO_3 \rightleftharpoons H^+ + HCO_3^- \quad \text{(Reaction 1)}$$

However, in the aqueous boundary layer and at the surface of dissolving drug, the reaction rate kinetics are critically important to consider and it was shown by Krieg et al.[17] that the CO_2–bicarbonate buffer behave according to Reaction (2).

$$CO_2\,(aq) + H_2O \leftarrow H_2CO_3 \rightleftharpoons H^+ + HCO_3^- \quad \text{(Reaction 2)}$$

In the diffusion layer, the reaction between CO_2 and H_2O to form carbonic acid occurs at a sufficiently slow rate that it will effectively not occur to a significant extent in the short residence time in the diffusion layer ($\leq$0.5 s). Therefore, the buffer capacity of bicarbonate in the diffusion layer will be governed by Reaction (2) (irreversible reaction rate model: IRR model). Because of the differences in these two reaction schemes, one can consider bicarbonate buffer as behaving as two different buffers: the bulk equilibrium buffer (Reaction (1)) and a dynamic, irreversible reaction rate buffer (IRR) in the diffusion layer. As a result of these considerations, low buffer capacities may be required by the equivalent phosphate buffer to match bicarbonate buffer, and external control of pH may be necessary to maintain the pH of the bulk solution.

This paper will experimentally examine the buffer effects of phosphate and bicarbonate using rotating disk dissolution of weak acid and weak base drugs and demonstrate a process for selecting an equivalent phosphate buffer based on drug solubility and pK_a properties. The experimental data will be compared with predictions and the results will show that the dissolution of both weak acid and weak base drugs can be accurately predicted in buffers with different physicochemical properties. Also, the dissolution data will illustrate the impact of the slow CO_2 hydration reaction and how matching other buffer systems to bicarbonate is more complex than simply matching bulk solution buffer capacities. These results may provide the basis for predicting phosphate buffer concentrations that are more indicative of the buffer present in the luminal fluid of the intestine and offer a more physiologically relevant dissolution buffer.

Applying a Simultaneous Diffusion and Reaction Model to Phosphate Buffer

Phosphate buffer properties are determined by the following ionization reactions:

$$H_3PO_4 \overset{K_{a1}}{\rightleftarrows} H_2PO_4^{-1} \quad pK_{a1} = 1.86 \quad \text{(Reaction 3)}$$

$$H_2PO_4^{-1} \overset{K_{a2}}{\rightleftarrows} HPO_4^{-2} \quad pK_{a2} = 6.8 \quad \text{(Reaction 4)}$$

$$HPO_4^{-2} \overset{K_{a3}}{\rightleftarrows} PO_4^{-3} \quad pK_{a3} = 11.5 \quad \text{(Reaction 5)}$$

At physiologically relevant pH values of the small intestine, the only relevant pK_a value is 6.8 (pK_{a2}) as demonstrated by Aunins et al.[2] who incorporated buffers with multiple pK_a values into the simultaneous diffusion and chemical reaction model. The values for pK_{a1} (1.86) and pK_{a3} (11.5) are not in the range of the physiologically relevant intestinal pH and therefore have no significant buffer effects. Therefore, the only species of relevance are monobasic phosphate and dibasic phosphate (Reaction (4)). This point stresses the importance of having pK_a values that are consistent with the properties used in the bulk solution. The ionic strength of the solution can alter the pK_a of a buffer or drug. Therefore, having measurements or literature values for pK_a at similar ionic conditions to the dissolution medium is important to assess how the buffer and drug will alter the pH in the diffusion layer. For Reactions (3)–(5), the reaction rates for ionization are assumed to be occurring so fast that they occur instantaneously relative to diffusion. Therefore, the film model accurately predicts the impact of phosphate buffer on the dissolution of weak acid drugs as described by Mooney et al.[19] and Aunins et al.[2]

In this paper, the same film model procedure is applied to weak base drugs. In contrast to a weak acid, a weak base drug will protonate at pH values below its pK_a and consequently it will produce OH^- in solution. As a result, the pH at the surface of a weak base drug will generally be higher than that of the bulk solution pH. Hence, the chemical equilibrium reactions must take this into account. The equilibrium reactions are shown below.

$$H^+ + OH^- \overset{K_w}{\rightleftarrows} H_2O \quad \text{(Reaction 6)}$$

$$B^- + H_2O \overset{K_b^D}{\rightleftarrows} BH + OH^- \quad \text{(Reaction 7)}$$

$$B^- + H^+ \overset{K_1^*}{\rightleftarrows} BH + H_2O \quad \text{(Reaction 8)}$$

$$B^- + H_2PO_4^- \overset{K_2}{\rightleftarrows} BH + HPO_4^{-2} \quad \text{(Reaction 9)}$$

$$HPO_4^{-2} + H_2O \overset{K_b^B}{\rightleftarrows} H_2PO_4^- + OH^- \quad \text{(Reaction 10)}$$

where B^- is the deprotonated form of the weak base drug and BH is the protonated form of the weak base drug.

The assumptions made in the film model for weak acids are applied here to weak bases for the first time with the chemical equilibrium adjusted accordingly. The main assumptions are that the species in the diffusion layer acting as acids must be equal to the species acting as bases, drug cannot be created or destroyed, and that charge neutrality is maintained throughout the diffusion layer. The assumptions simplify the differential equations and allow for the pH at the surface to be calculated. For example, the electrical neutrality assumption is defined by setting the sum of the flux of the negatively charged species equal to the sum of the flux of the positively charged species. These assumptions couple diffusion and charge neutrality. There is also an assumption that the diffusion coefficient of each species is the same in the bulk solution as it is in the diffusion layer. Literature has shown that this assumption may not be accurate as varying the concentration of ions in solution can impact the diffusivity of a species.[20] However, the bulk solution was made isotonic by adding sodium chloride. This should make the concentration of ions relatively constant throughout because the presence of the drug in the diffusion layer will only minimally change the total ion concentration.

Solving the associated differential equations in the manner of Mooney et al.,[19] a cubic equation can be obtained for the OH^- concentration at the surface of the tablet that then allows the pH at the surface of the tablet to be calculated. This cubic equation is shown below.

$$p[\mathrm{OH^-}]_0^3 + q[\mathrm{OH^-}]_0^2 + r[\mathrm{OH^-}]_0 + s = 0 \tag{1}$$

$$p = D_{\mathrm{OH}} D_{\mathrm{HPO_4}}$$

$$q = D_{\mathrm{OH}} D_{\mathrm{H_2PO_4}} K_b^B + D_{\mathrm{HPO_4}} D_H \left[\mathrm{H^+}\right]_h + D_{\mathrm{HPO_4}} D_{\mathrm{H_2PO_4}} \left[\mathrm{H_2PO_4^-}\right]_h - D_{\mathrm{HPO_4}} D_{\mathrm{OH}} \left[\mathrm{OH^-}\right]_h$$

$$r = D_{\mathrm{H_2PO_4}} D_H K_b^B \left[\mathrm{H^+}\right]_h + D_{\mathrm{H_2PO_4}}^2 K_b^B \left[\mathrm{H_2PO_4^-}\right]_h - D_{\mathrm{H_2PO_4}} D_{\mathrm{OH}} K_b^B \left[\mathrm{OH^-}\right]_h - D_{\mathrm{H_2PO_4}}^2 K_b^B \left[\mathrm{H_2PO_4^-}\right]_h - D_{\mathrm{H_2PO_4}} D_{\mathrm{HPO_4}} K_b^B \left[\mathrm{HPO_4^{-2}}\right]_h - D_{\mathrm{BH}} D_{\mathrm{HPO_4}} K_b^D \left[B^-\right]_0 - D_H D_{\mathrm{HPO_4}} K_w$$

$$s = -D_{\mathrm{BH}} D_{\mathrm{H_2PO_4}} K_b^D K_b^B \left[B^-\right]_0 - D_H D_{\mathrm{H_2PO_4}} K_w K_b^B$$

This same transport analysis assuming instantaneous chemical equilibrium may be applied to bicarbonate buffer as described by Krieg et al.[17] The BCE model assumes that the hydration and dehydration reactions in the formation of bicarbonate are fast enough to reach chemical equilibrium instantaneously (Reaction (1)): $pK_a = 6.04$). The carbonic acid ionization (CAI) model assumes that the hydration and dehydration reactions are too slow to occur at all in the diffusion layer ($H_2CO_3H^+ + HCO_3^-$: $pK_a = 3.55$). A thorough explanation of these models for weak acid drugs is given in Krieg et al.[17]

Applying a Simultaneous Diffusion and Reaction Model with an Irreversible Chemical Reaction to Weak Base Drugs

The IRR model reaction scheme represented in Reaction (2) from Krieg et al.[17] to predict weak acid dissolution was used to analyze the impact of the slow hydration and dehydration reactions on bicarbonate buffer by assuming that H_2CO_3 undergoes an irreversible chemical reaction to form CO_2 and H_2O. The chemical reactions that were considered for the weak base dissolution analysis are shown below:

$$\mathrm{H^+ + OH^- \overset{K_w}{\rightleftarrows} H_2O} \qquad \text{(Reaction 11)}$$

$$\mathrm{B^- + H_2O \overset{K_b^D}{\rightleftarrows} BH + OH^-} \qquad \text{(Reaction 12)}$$

$$\mathrm{B^- + H^+ \overset{K_1^+}{\rightleftarrows} BH + H_2O} \qquad \text{(Reaction 13)}$$

$$\mathrm{B^- + H_2CO_3 \overset{K_2}{\rightleftarrows} BH + HCO_3^-} \qquad \text{(Reaction 14)}$$

$$\mathrm{HCO_3^- + H_2O \overset{K_b^B}{\rightleftarrows} H_2CO_3 + OH^-} \qquad \text{(Reaction 15)}$$

$$\mathrm{H_2CO_3 \overset{k_d}{\rightleftarrows} CO_2 + H_2O} \qquad \text{(Reaction 16)}$$

The impact of dehydration reaction rate (k_d) in the calculation for the hydroxide ion concentration at the surface of the dissolving drug appears in Eq. (2). In this model, a simplifying assumption is that the hydration reaction rate equals zero.

$$p\left[\mathrm{OH^-}\right]_0^3 + q\left[\mathrm{OH^-}\right]_0^2 + r\left[\mathrm{OH^-}\right]_0 + s = 0 \tag{2}$$

$$p = -D_{\mathrm{HCO_3}} D_{\mathrm{OH}}$$

$$q = -D_{\mathrm{HCO_3}} D_H \left[\mathrm{H^+}\right]_h + D_{\mathrm{HCO_3}} D_{\mathrm{OH}} \left[\mathrm{OH^-}\right]_h - \left(h\sqrt{D_{\mathrm{H_2CO_3}} k_d}\right) K_b^B D_{\mathrm{OH}} - \left(h\sqrt{D_{\mathrm{H_2CO_3}} k_d}\right) D_{\mathrm{HCO_3}} \left[\mathrm{H_2CO_3}\right]_h$$

$$r = D_{\mathrm{HCO_3}} D_{\mathrm{BH}} K_b^D \left[B^-\right]_0 - \left(h\sqrt{D_{\mathrm{H_2CO_3}} k_d}\right) K_b^B D_H \left[H^+\right]_h + D_{\mathrm{HCO_3}} D_H K_W + \left(h\sqrt{D_{\mathrm{H_2CO_3}} k_d}\right) K_b^B D_{\mathrm{OH}} \left[\mathrm{OH^-}\right]_h + \left(h\sqrt{D_{\mathrm{H_2CO_3}} k_d}\right)^2 K_b^B \left[\mathrm{H_2CO_3}\right]_h + \left(h\sqrt{D_{\mathrm{H_2CO_3}} k_d}\right) D_{\mathrm{HCO_3}} K_b^B \left[\mathrm{HCO_3^-}\right]_h - \left(h\sqrt{D_{\mathrm{H_2CO_3}} k_d}\right)^2 K_b^B \left[\mathrm{H_2CO_3}\right]_h$$

$$s = \left(h\sqrt{D_{\mathrm{H_2CO_3}} k_d}\right) D_{\mathrm{BH}} K_b^D K_b^B \left[B^-\right]_0 + \left(h\sqrt{D_{\mathrm{H_2CO_3}} k_d}\right) D_H K_w K_b^B$$

MATERIALS AND METHODS

Benzoic acid (Sigma–Aldrich, St. Louis, Missouri; >99.5%, lot #MKBG2270V), ibuprofen (Albermarle, Baton Rouge, Louisiana; lot #11550-0005), indomethacin (Alexis Biochemicals, San Diego, California; ≥98%, lot #L25666), 2-napthoic acid (Sigma–Aldrich; lot #14709KHV), ketoprofen (Sigma–Aldrich; lot #044K0790), and Haloperidol (TCI, Portland, Oregon; >98.0% lot #D6C3D-R1) were used as received. All other chemicals used were of analytical grade. Distilled water was

Table 1. Rotating Disk Dissolution Experimental Parameters Applied to the Weak Acid Drugs Examined at 37°C and Isotonic Solution (Ionic Strength = 0.154 mol/L)

Drug	Ibuprofen	Indomethacin	Ketoprofen	2-Naphthoic Acid	Benzoic Acid
Bulk pH	6.5	6.5	6.5	6.5	6.5
Percent CO_2	7–8	7–8	7–8	7–8	6.5–7.5
	14–16	14–16	14–16	14–16	11–13
	21–22	21–22	24–26	22–25	25–27
					33–37
Total buffer concentration $[CO_2(aq)]+[HCO_3^-]$ (mM)	6.5–7.5	6.5–7.5	6.5–7.5	6.5–7.5	6–7
	13–15	13–15	13–15	13–15	10.3–12.1
	19.5–20.5	19.5–20.5	22–24	20.5–23.5	23.3–25.2
					30.8–34.5
$[CO_2(aq)]+[HCO_3^-]$	2.9–3.3	2.9–3.3	2.9–3.3	2.9–3.3	2.7–3.1
Bulk solution	5.7–6.6	5.7–6.6	5.7–6.6	5.7–6.6	4.5–5.3
Buffer capacity dn/dpH(mM/ΔpH)	8.6–9.0	8.6–9.0	9.8–10.7	9.0–10.3	10.3–11.1
					13.5–15.2
Bicarbonate concentration $[HCO_3^-]$ (mM)	5–5.5	5–5.5	5–5.5	5–5.5	4.5–5.2
	10–11	10–11	10–11	10–11	7.6–9.0
	14.5–15.5	14.5–15.5	16.5–18.0	15–17	17.3–18.7
					22.9–25.6
Phosphate buffer concentration $[H_2PO_4^-]+[HPO_4^{-2}]$ (mM)	3.5	2.5	10	10	13
	5.2	13	25	25	25
	6.95	25	50	50	43.5
	13	43.5			
	25				
	43.5				
Phosphate buffer	1.79	1.28	5.12	5.12	6.66
Bulk solution buffer capacity dn/dpH(mM/ΔpH)	2.66	6.66	12.81	12.81	12.81
	3.56	12.81	25.61	25.61	22.28
	6.66	22.28			
	12.81				
	22.28				
Volume of dissolution medium (mL)	150	100	300	200	300
rpm	100	100	100	100	100

used for all experiments. All dissolution runs were performed in a jacketed beaker at 37°C. Two dissolution runs were carried out for each experimental condition described below. Samples were analyzed using a UV spectrophotometer (Agilent Technologies, Santa Clara, California; model #61103A). The samples were obtained using a flow-through system that recycled the analyzed solution back into the dissolution vessel. The standard curves were also made using the UV flow through system.

Dissolution experiments using phosphate buffer were performed in duplicate at pH 6.5 at several different phosphate concentrations and medium volumes. The exact experimental parameters can be seen in Tables 1 and 2. Solutions were made using sodium monobasic phosphate, sodium hydroxide, and sodium chloride so the ionic strength of the buffer solution was isotonic. A disc of compressed drug with a tablet diameter of 1 cm was used for ibuprofen, indomethacin, ketoprofen, and haloperidol. A compressed disc with a tablet diameter of 0.472 cm was used for benzoic acid and 2-naphthoic acid. Differences in volume and tablet diameter used for these experiments were made according to the solubility and predicted flux of each drug to achieve desirable experimental conditions (sink conditions and adequate sensitivity for UV analysis). All experiments were carried out at 100 rpm.

For the rotating disk dissolution experiments in bicarbonate buffer, different bicarbonate buffer concentrations were prepared by continuously flowing quantities of 100% dry compressed air and 100% carbon dioxide in a 0.9% NaCl solution at appropriate ratios directly into the distilled water. The $\%CO_2(aq)$ in solution was determined using a CO_2 monitor (YSI 8500, Yellow Springs, Ohio) and pH was monitored using a pH meter (Beckman Φ 40, Brea, California). Solid sodium hydroxide or 5N NaOH was added to adjust pH. The exact experimental parameters can be seen in Tables 1 and 2. Note that the buffer concentration may be defined either as the bicarbonate concentration or the sum of bicarbonate and CO_2 as shown in Tables 1 and 2.

The solubility of 2-naphthoic acid was determined by agitating the suspension in 0.1N hydrochloric acid solution while being kept at 37°C. Samples were filtered before dilution in pH 6.5, 50 mM phosphate buffer.

The flux of the drugs was predicted by applying the mathematical models outlined in this paper and in Krieg et al.[17] using MATLAB (Mathworks, Natick, Massachusetts). The drug and

Table 2. Rotating Disk Dissolution Experimental Parameters Applied to the Weak Base Drug Haloperidol at 37°C and Isotonic Solution (Ionic Strength = 0.154 mol/L)

Drug	Haloperidol		
Bulk pH	6.0	6.5	7.0
Percent CO_2	45	7–8	5
		14–16[a]	
		22	
Total buffer concentration $[CO_2(aq)]+[HCO_3^-]$ (mM)	20.7	6.5–7.5	12.2
		13–15[a]	
		20.5	
Bicarbonate concentration $[HCO_3^-]$ (mM)	9.9	5–5.5	11
		10–11[a]	
		15	
$[CO_2(aq)]+[HCO_3^-]$	11.9	2.9–3.3	2.5
Bulk solution		5.7–6.6	
Buffer capacity dn/dpH(mM/ΔpH)		9.0	
Phosphate buffer concentration $[H_2PO_4^-+HPO_4^{-2}]$ (mM)	NA	2.5	NA
		13	
		25	
		43.5	
Phosphate buffer	NA	1.28	NA
Bulk solution buffer capacity dn/dpH(mM/ΔpH)		6.66	
		12.81	
		22.28	
Volume of dissolution medium (mL)	75	75	75
rpm	100	100	100

[a]Experimental parameters that were used for pH 6.5 in bicarbonate buffer in Figure 7.

buffer properties that were applied to the analysis are given in Table 3. The predictions using the IRR and CAI models had a buffer concentration input equal to the bicarbonate concentration. When the BCE model was applied to bicarbonate buffer, the buffer concentration was equal to the sum of bicarbonate and CO_2 concentrations. This is because of the assumptions of each model.

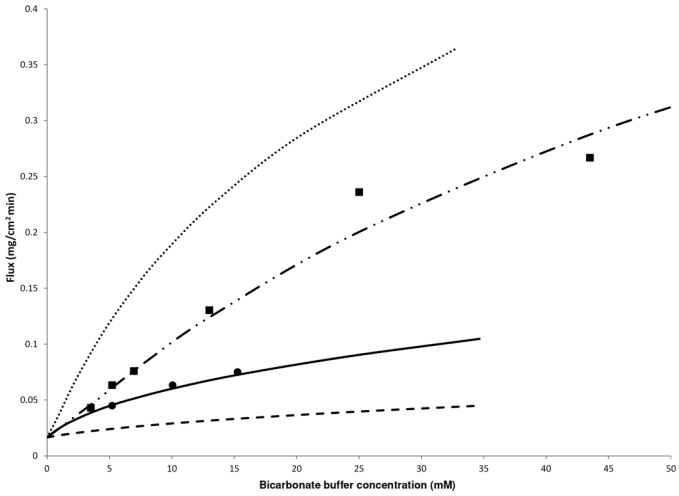

Figure 1. The experimental and predicted flux of ibuprofen in bicarbonate and phosphate buffer at multiple concentrations (at pH 6.5 and 37°C). Key: (■) experimental flux in phosphate buffer; (▬ ▪ ▪) predicted flux in phosphate buffer (BCE); (●) experimental flux in bicarbonate buffer; (▪▪▪▪▪▪▪▪▪) BCE model flux predictions; (▬▬▬▬) IRR model flux predictions; (▬ ▬ ▬) CAI model flux predictions.

RESULTS

Ibuprofen Results

Figure 1 shows the flux of ibuprofen in phosphate buffer over a range of buffer concentrations along with theoretical predictions for each model at pH 6.5. The data for the flux of ibuprofen, in bicarbonate buffer, are also included for comparison purposes and are described in detail in Krieg et al.[17] The rotating disk flux of ibuprofen in phosphate buffer is accurately predicted by the simultaneous diffusion and chemical reaction model as expected. The predictions show that an increase in phosphate buffer concentration results in a significant increase in the flux but ibuprofen still serves as a self-buffer and influences surface pH under the conditions studied. Figure 1 shows that the phosphate buffer concentrations needed to match ibuprofen

Table 3. Drug and Buffer Properties Applied to the Different Mathematical Models

Species	Intrinsic Solubility at 37°C (mol/L)	pK_a	Diffusion Coefficient (cm^2/s)	Ionic Strength/ Temperature Conditions for the pK_a Values Listed
Benzoic acid	0.0334[21]	4.19[22]	12.0×10^{-6}[a]	Water/25°C[22]
Ibuprofen	3.30×10^{-4}[18]	4.43[18]	7.93×10^{-6}[a]	0.15/37°C[18]
Indomethacin	5.963×10^{-6}[b]	4.27[23]	$6.8 \times 10-6$[24]	0.15/37°C[23]
Ketoprofen	5.303×10^{-4}[b]	4.02[25]	$9.3 \times 10-6$[4]	0.15/37°C[25]
2-Napthoic acid	3.044×10^{-4}[b]	4.22[26]	9.86×10^{-6}[a]	0.02/25°C[26]
Haloperidol	3.518×10^{-6}[25]	8.35[25]	6.6×10^{-6}[24]	0.15/37°C[25]
Phosphate		6.8[18]	11.5×10^{-6}[4]	0.15/37°C[18]
Bicarbonate		6.04[b,c]	14.6×10^{-6}[27]	0.15/37°C[b]
Carbonic acid		3.55[28d]	14.6×10^{-6}[27]	0.217/37°C[28]
Carbon dioxide	0.02403[17]		24.9×10^{-6}[29]	

Values were taken from literature. Haloperidol solubility and pK_a data were taken from USP (2000)[5] and used to calculate the intrinsic solubility of haloperidol based on their reported measured solubility in a pH 4.94 saturated solution.

[a]Diffusion coefficients were estimated using the Wilke–Chang equation,[30] or [b]measured experimentally.

[c]Chemical equilibrium: $CO_2(aq) + H_2O \rightleftarrows^{K_a} H^+HCO_3^-$.

[d]Carbonic acid chemical equilibrium $H_2CO_3 \rightleftarrows^{K_{a1}} H^+ + HCO_3^-$.

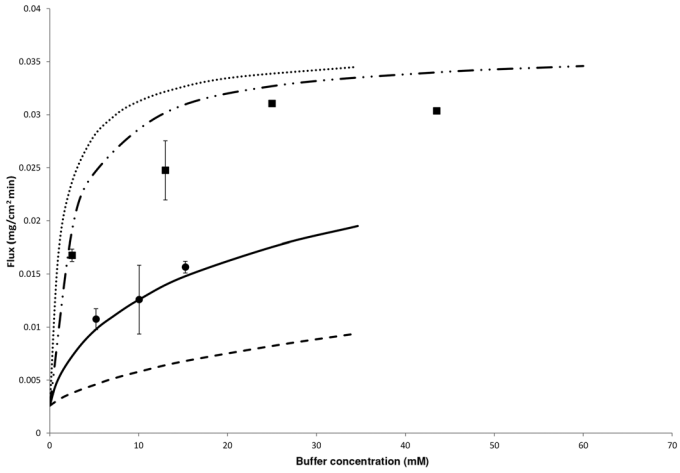

Figure 2. The experimental and predicted flux of indomethacin in bicarbonate and phosphate buffer at multiple concentrations (at pH 6.5 and 37°C). Key: (■) experimental flux in phosphate buffer; (▬ ▪ ▪) predicted flux in phosphate buffer (BCE); (●) experimental flux in bicarbonate buffer; (••••••••••) BCE model flux predictions; (▬▬▬) IRR model flux predictions; (▬ ▬ ▬) CAI model flux predictions.

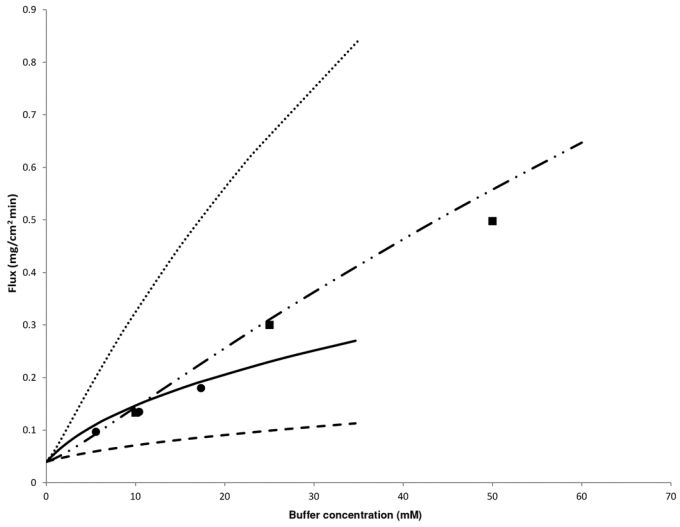

Figure 3. The experimental and predicted flux of ketoprofen in bicarbonate and phosphate buffer at multiple concentrations (at pH 6.5 and 37°C). Key: (■) experimental flux in phosphate buffer; (▬ ▪ ▪) predicted flux in phosphate buffer (BCE); (●) experimental flux in bicarbonate buffer; (••••••••••) BCE model flux predictions; (▬▬▬) IRR model flux predictions; (▬ ▬ ▬) CAI model flux predictions.

dissolution in physiologically relevant bicarbonate buffer are 4–8 mM.

Indomethacin Results

Figure 2 shows the flux of indomethacin in bicarbonate and phosphate buffer over a range of buffer concentrations along with theoretical predictions at pH 6.5. The data for the flux of indomethacin, in bicarbonate buffer, are described in detail in Krieg et al.[17] The simultaneous diffusion and chemical reaction (BCE) model accurately predicts the experimental flux of indomethacin in phosphate buffer. The calculated pH at the surface of indomethacin approaches the bulk pH at low concentrations of phosphate buffer as expected because of the low-intrinsic solubility of indomethacin that makes it a poor self-buffer. Bicarbonate is not able to buffer the surface pH of indomethacin as effectively as phosphate buffer. Therefore, very low phosphate buffer concentrations (1–2 mM) are needed to match physiologically relevant bicarbonate buffer. As was seen for ibuprofen, the slow hydration reaction rate has a significant impact on the buffer capacity of bicarbonate and only the IRR model can accurately predict the flux of indomethacin in bicarbonate buffer.

Ketoprofen Results

Figure 3 shows the flux of ketoprofen in bicarbonate and phosphate buffer over a range of buffer concentrations along with theoretical predictions at pH 6.5. The data for the flux of ketoprofen, in bicarbonate buffer, is described in detail in Krieg et al.[17] The predictions show that an increase in buffer concentration results in a significant increase in the flux. The predicted flux matches the experimental flux in phosphate buffer. The experimental flux of ketoprofen in bicarbonate buffer is only accurately predicted when the IRR model is applied. Figure 3 shows that phosphate buffer concentrations needed to match physiologically relevant bicarbonate buffer are approximately 5–12 mM.

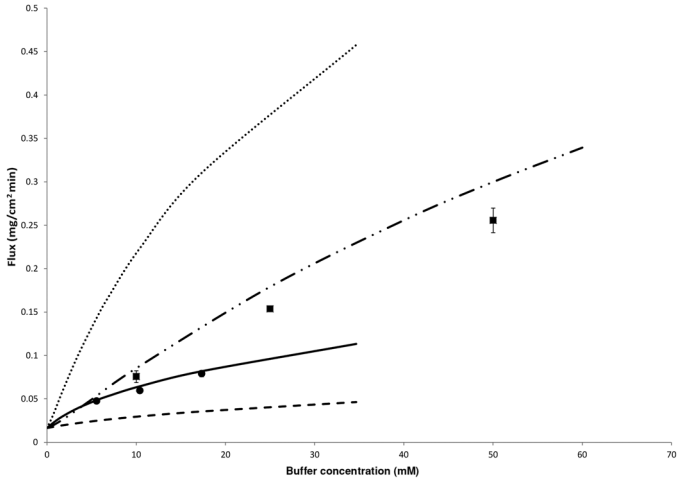

Figure 4. The experimental and predicted flux of 2-napthpoic acid in bicarbonate and phosphate buffer at multiple concentrations (at pH 6.5 and 37°C). Key: (■) experimental flux in phosphate buffer; (▬ ▪ ▪) predicted flux in phosphate buffer (BCE); (●) experimental flux in bicarbonate buffer; (••••••••••) BCE model flux predictions; (▬▬▬) IRR model flux predictions; (▬ ▬ ▬) CAI model flux predictions.

2-Napthoic Acid Results

Figure 4 shows the flux of 2-napthoic acid in bicarbonate and phosphate buffer over a range of buffer concentrations along with theoretical predictions at pH 6.5. The predictions show that an increase in buffer concentration results in a significant increase in the flux. The solubility of 2-naphthoic acid is similar to ibuprofen. Therefore, 2-napthoic acid acts similarly as a self-buffer at the dissolving surface. The predicted flux matches the experimental flux in phosphate buffer. The experimental flux of 2-naphthoic acid in bicarbonate buffer is only accurately predicted when the dehydration reaction rate is incorporated by applying the IRR model. Figure 4 shows phosphate buffer

concentrations needed to match physiologically relevant bicarbonate buffer are similar to ibuprofen (3–10 mM).

Benzoic Acid

Figure 5 shows the flux of benzoic acid in bicarbonate and phosphate buffer over a range of buffer concentrations at pH 6.5. The flux of benzoic acid in phosphate buffer is accurately predicted by the simultaneous diffusion and chemical reaction model. The predictions and results show that a large increase in buffer concentration does not cause a significant increase in the flux. This is because of the high solubility of benzoic acid that is apparent in the large flux value for benzoic acid at zero buffer concentration. A highly soluble weak acid drug will lead to a high concentration of drug at the surface and a high $[H^+]$ that limits the pH change at the surface even in the presence of high-buffer concentration. In effect, the solubility of benzoic acid very effectively serves as a self-buffer and controls surface pH under the conditions studied.

As observed with all of the weak acid drugs, the BCE and CAI models do not accurately predict the flux of benzoic acid in bicarbonate buffer. In the case of benzoic acid dissolution in bicarbonate buffer, it was observed throughout these experiments that gas bubbles continuously formed at the surface of the dissolving tablet. This very likely affected the hydrodynamics and effective surface area of the dissolving drug available for dissolution resulted in a poor correlation with the IRR model. The gas bubbles at the dissolving surface were likely carbon dioxide. The concentration of CO_2 at the surface depends on the $[H^+]$ concentration Eq. (3). When $[H^+]$ is sufficiently high, the CO_2 (aq) concentration can exceed its solubility under the conditions studied and cause CO_2 to come out of solution.

$$\left[CO_2\,(aq)\right] = \frac{\left[H^+\right]\left[HCO_3^-\right]}{K_{a1}} \tag{3}$$

The BCE model enables the calculation of the concentration of carbon dioxide at the surface of the tablet. At the highest experimental CO_2 partial pressure (37% CO_2), the BCE model predicts a nearly saturated solution (98% saturated) of CO_2 at the surface of the tablet. Furthermore, the assumptions made in the IRR model are consistent with the buildup of carbon dioxide in the diffusion layer. The IRR model assumes that the concentration of carbon dioxide will only increase in the diffusion layer without an ability to be transformed back into carbonic acid. Additionally, the high solubility of benzoic acid leads to a low pH in the diffusion layer that will generate more carbon dioxide and could cause the concentration of carbon dioxide to exceed its solubility. Hence, these predictions are very consistent with the IRR model and the hypothesis that the bubbles formed at the dissolving benzoic acid compact surface are because of saturated CO_2 conditions in the diffusion layer and at the dissolving surface.

Haloperidol Results

Figure 6 shows haloperidol flux, a weak base, in bicarbonate and phosphate buffer over a range of buffer concentrations at pH 6.5. The predictions show that an increase in buffer concentration results in a significant increase in the flux. The solubility of haloperidol is similar to indomethacin and, in the same way, the low solubility of the drug prevents it from effectively self-buffering the surface pH. The rotating disk experimental flux in phosphate buffer is predicted accurately by the BCE model. The experimental flux of haloperidol in bicarbonate buffer falls between the BCE model ($pK_a = 6.04$) and the CAI model ($pK_a = 3.55$). Experimental flux of haloperidol in bicarbonate buffer is only accurately predicted when the IRR model is used for the predictions. The data and predictions show that for low-solubility drugs, such as haloperidol, it is important to have accurate physicochemical properties to make accurate predictions. The parameters used for the haloperidol predictions were obtained from literature and the solubility and pK_a of haloperidol varies significantly in literature.[24,25,31–33] Additionally, the experimental data and predictions in bicarbonate and phosphate buffer show that phosphate is much better at

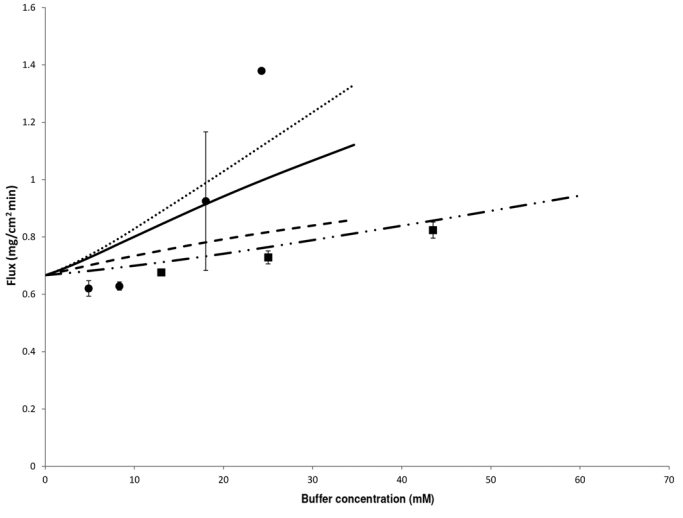

Figure 5. The experimental and predicted flux of benzoic acid in bicarbonate and phosphate buffer at multiple concentrations (at pH 6.5 and 37°C). Key: (■) experimental flux in phosphate buffer; (▬ ▪ ▪) predicted flux in phosphate buffer (BCE); (●) experimental flux in bicarbonate buffer; (••••••••••) BCE model flux predictions; (▬▬▬) IRR model flux predictions; (▬ ▬ ▬) CAI model flux predictions.

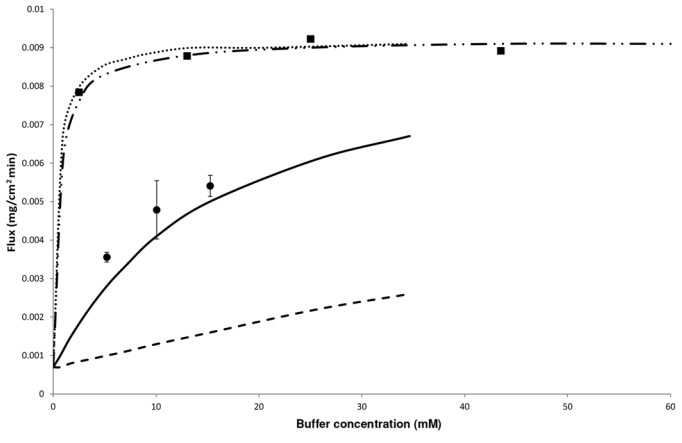

Figure 6. The experimental and predicted flux of haloperidol in bicarbonate and phosphate buffer at multiple concentrations (at pH 6.5 and 37°C). Key: (■) experimental flux in phosphate buffer; (▬ ▪ ▪) predicted flux in phosphate buffer (BCE); (●) experimental flux in bicarbonate buffer; (••••••••••) BCE model flux predictions; (▬▬▬) IRR model flux predictions; (▬ ▬ ▬) CAI model flux predictions.

 DOI 10.1002/jps.24460

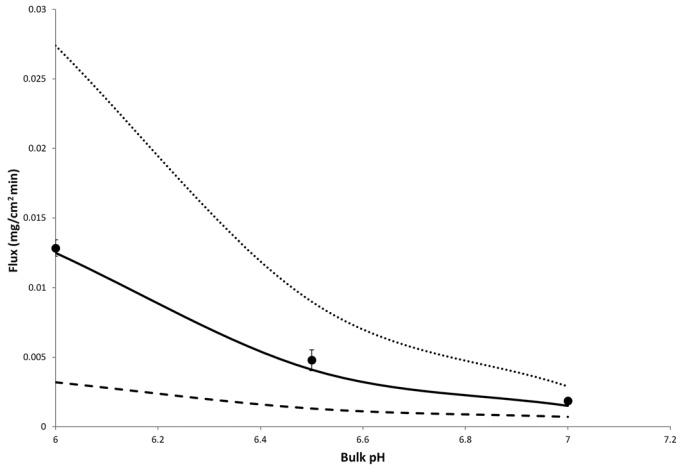

Figure 7. The experimental and predicted flux of haloperidol in approximately 10 mM bicarbonate buffer at bulk pH values 6, 6.5, and 7 at 37°C. Key: (●) experimental flux; (••••••••••) BCE model flux predictions; (——————) IRR model flux predictions; (— — —) CAI model flux predictions.

buffering the surface pH. Therefore, very low concentrations of phosphate buffer would be needed to match bicarbonate (<1 mM).

Figure 7 shows the experimental and predicted flux of haloperidol in 10 mM bicarbonate buffer with bulk pH values of 6, 6.5, and 7. As the bulk pH decreases, the experimental and predicted flux in bicarbonate increases. This is because of an increase in H^+ in the solution and consequently a decrease in the surface pH and an increase in the ionized form of the drug in the diffusion layer, leading to an increase in the overall flux of the weak base drug. The BCE model overestimates and the CAI model underestimates the effect that changing the bulk pH will have on the surface pH and the flux of the drug. The IRR model accurately predicts experimental flux of haloperidol in bicarbonate buffer.

DISCUSSION

The dissolution data presented here for weak acid and weak base drugs illustrate the importance the reaction rates play in the buffering capacity of bicarbonate in the diffusion layer. If the hydration and dehydration reaction were effectively instantaneous, the dissolution in bicarbonate would have been predicted to be faster than the dissolution in phosphate buffer in accordance with the BCE model. As the pH in the diffusion layer would be lower than 6.5 because of the ionization/dissolution of the weak acid drug, the pK_a of bicarbonate of 6.04 would make it a better buffer than the phosphate buffer with a pK_a of 6.8 at the dissolving drug surface. The predicted curves comparing the BCE bicarbonate buffer model and the BCE phosphate buffer model demonstrate this. Therefore, matching the buffer capacity of two different buffers in the bulk solution will not result in the same dissolution profile because the drug itself plays an important role in the dissolution rate. For example, a buffer concentration of 15 mM CO_2–bicarbonate buffer in the bulk solution at pH 6.5 has the same buffer capacity as 13 mM phosphate buffer at pH 6.5 in the bulk solution. However, the predictions and experimental results show that matching these buffer capacities will not lead to matching dissolution rates.

When the slow-hydration reaction of bicarbonate is assumed to be insignificant in the CO_2–bicarbonate buffer system, as it is in the IRR model, the dissolution all the weak acid and weak base drugs studied here in bicarbonate buffer is accurately predicted. The impact of the slow hydration reaction is significant and drastically alters the buffer capacity of the CO_2–bicarbonate buffer system in the diffusion layer adjacent to the surface of the drug. Comparing the predictions for the BCE and IRR transport analysis reaction schemes for the CO_2–bicarbonate buffer demonstrates the dynamic nature of bicarbonate buffer. For example, the BCE bicarbonate model would predict that a 10-mM bicarbonate buffer would provide the same buffering ability in the diffusion layer as approximately 50 mM phosphate buffer at a bulk of pH 6.5. Therefore, when the reaction time is unlimited (i.e., in the bulk solution) and the rates of the hydration and dehydration reactions do not play a limiting role in buffering capacity (i.e., the BCE model), bicarbonate acts as a strong buffer. However, when a drug is dissolving and there is a finite reaction time (i.e., in the diffusion layer using the IRR model), bicarbonate has a much lower buffer capacity that is only partially compensated for by the dehydration of H_2CO_3. This transport/reaction analysis indicates that bicarbonate is very effective at minimizing changes in the bulk aqueous phase (e.g., in the intestinal lumen), but the effectiveness of bicarbonate as a buffer becomes significantly altered in the diffusion layer for dissolving weak acid and weak base drugs at intestinal pH values.

The flux data also confirms that the IRR model accurately predicts the experimental flux of weak acid drugs in bicarbonate buffer. It can also be applied to weak base drugs at different buffer concentrations and bulk pH. This has not been previously shown and is important because many drugs are weak bases and provides insight into the dissolution of weak bases in the intestine. Furthermore, the experimental data for haloperidol and the data presented in Krieg et al.[17] demonstrate the ability of the IRR model to be used under various experimental conditions (e.g., different bulk pH, drug solubilities, rotational speeds). Results also give good approximations of the phosphate buffer concentrations needed to match physiologically relevant bicarbonate buffer concentrations for rotating disk dissolution of drugs with varying physiochemical properties. For the drugs studied in this paper, the phosphate buffer concentrations needed to match physiologically relevant bicarbonate buffer were approximately 1–15 mM based on the experimental data and the IRR model predictions.

Additionally, the data in phosphate buffer further confirm the accuracy of the film model to predict the dissolution of weak acid drugs in phosphate buffer and that it can be successfully applied to weak base drugs that had not been previously shown.

Predicting Physiologically Relevant Phosphate Buffer Concentrations

Although there have been recent advancements in preparing bicarbonate buffer and controlling buffer concentration,[34] the process of making bicarbonate buffer is not ideal for performing dissolution experiments. The experimental data in this paper and the data in Krieg et al.[17] demonstrate that the IRR model can accurately predict the effect bicarbonate has on buffering surface pH of weak acid and weak base drugs under rotating disk dissolution conditions. This paper and previous work also illustrates the ability to accurately predict rotating disk drug

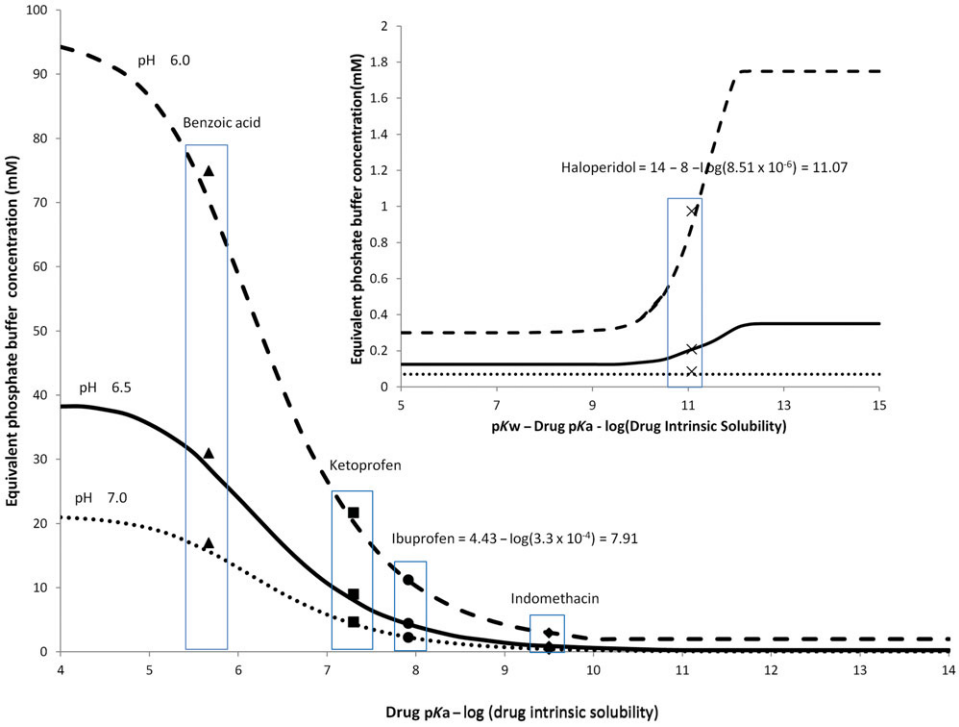

Figure 8. The predicted equivalent phosphate buffer concentration needed to match 10.5 mM bicarbonate buffer for weak acid drugs with drug pK_as of 3–8 and weak base drugs with pK_as of 5–10 and drug solubilities of 0.1–10^{-6} M for both. Key: (▬ ▬ ▬) equivalent buffer predictions at pH 6 (h = 30 μm); (▬▬▬) equivalent buffer predictions at pH 6.5 (h = 30 μm); (••••••••••) equivalent buffer predictions at pH 7 (h = 30 μm); (▲) equivalent buffer predictions for benzoic acid; (■) equivalent buffer predictions for ketoprofen; (●) equivalent buffer predictions for ibuprofen; (♦) equivalent buffer predictions for indomethacin; (X) equivalent buffer predictions for haloperidol.

dissolution in phosphate buffer using the film model assuming chemical equilibrium is achieved instantaneously.[2,4] Therefore, applying each of these models to their respective buffer system will provide accurate estimations for phosphate buffer concentrations that will simulate physiologically relevant bicarbonate buffer.

To estimate phosphate buffer concentrations needed to match physiologically relevant bicarbonate buffer, drug pK_a and solubility were varied and the IRR model was applied assuming an aqueous diffusion coefficient of 7.9×10^{-6} cm^2/s. For weak acids, the drug pK_a was varied from 3 to 8, and for weak bases the drug pK_a was varied from 5 to 10. The drug solubility was varied from 10^{-1} to 10^{-6} M. The physiologically relevant bicarbonate buffer chosen for the predictions was 15% CO_2 (10.4 mM bicarbonate concentration) at pH 6.5 as representative of small intestinal conditions.[35] The diffusion layer thickness for these predictions was chosen as 30 μm based on the work of Hintz and Johnson.[36]

The relationship between equivalent phosphate buffer concentration and the pK_a of weak acid drugs, pK_w–pK_a for weak base drugs, and log(drug solubility) is shown in Figure 8. For weak acid drugs, when the [pK_a–log(drug solubility)] is plotted versus the equivalent phosphate buffer concentration necessary to match physiologically relevant bicarbonate buffer, a single curve is obtained at each bulk pH as shown in Figure 8. The same is true for weak base drugs when [pK_w−pK_a−log(drug solubility)] is plotted versus equivalent phosphate buffer as shown in Figure 8. This is because of the relationship between the weak acid drug K_a (for a weak base: K_w−K_a) and the solubility of the drug in the cubic equation of the IRR model. These two parameters only appear in the cubic equation as being multiplied together. Therefore, if one parameter is decreased by an order of magnitude while the other is increased by an order of magnitude, this will result in the same solution for the cubic equation and pH at the surface of the drug. This figure provides an overview of the impact of drug solubility, pK_a, and bulk pH under what could be considered physiologically relevant buffer concentrations in the intestinal tract.

Predictions at bulk pH of 6.0, 6.5, and 7.0 show that phosphate buffer concentrations needed to match physiologically relevant bicarbonate buffer are higher for both weak acid and weak base drugs at pH 6 and lower at pH 7. This is because of the low pK_a for the ionization reaction of carbonic acid (pK_a = 3.55), which is used in the IRR model. As the bulk pH is lowered toward 3.55, the buffering capacity of bicarbonate increases. This is evident in the case of weak acid drugs. There is, however, a wide range of equivalent phosphate buffer concentrations needed to match weak acid drugs (~1–95 mM) depending on the bulk pH and drug properties (i.e., solubility and pK_a). As the drug pK_a increases and the drug solubility decreases for weak acid drugs, the phosphate buffer concentration needed to provide the same buffer effect decreases. However, when considering representative BCS class 2a drugs, such as ketoprofen, ibuprofen, and indomethacin shown in Figure 8, the equivalent phosphate buffer concentrations fall into the range of 1–25 mM. For example, ibuprofen is predicted to require an equivalent phosphate buffer concentration of approximately 11 mM at pH 6 and approximately 2 mM at pH 7.

In the case of weak base drugs, the matching phosphate buffer concentration for physiologically relevant bicarbonate

 DOI 10.1002/jps.24460

buffer is less than 2 mM for all drug pK_a values and solubilities evaluated. This is because of weak base drugs forming OH^- at the surface of the dissolving drug that increases the pH and makes the bicarbonate buffer relatively ineffective. The CAI reaction pK_a is much lower than the pH at the surface so the irreversible reaction provides only a minor increase in buffer capacity and makes bicarbonate a very poor buffer for weak base drugs. Therefore, very little phosphate buffer concentration is needed to decrease the pH at the surface of the dissolving weak base drug to have the same effect as physiologically relevant bicarbonate buffer.

The predictions of phosphate buffer concentrations that match physiologically relevant bicarbonate buffer offer a dissolution medium that can better simulate the impact of bicarbonate in the small intestine. The phosphate concentrations needed are both drug and pH dependent. Therefore, based on this work, each drug will require a phosphate buffer concentration dependent upon its properties. However, given the intrinsic solubility and the pK_a of the drug, this work allows for an estimate of a phosphate buffer concentration necessary to match dissolution in bicarbonate buffer.

The plots for equivalent phosphate buffer are made assuming an idealized experimental situation where the pH in the bulk solution and the diffusion layer thickness are constant. However, for particle dissolution, this may not be the case. As a weak acid or weak base drug dissolves, the bulk pH may change, especially in cases of high-dose drugs. Although the CO_2–bicarbonate buffer may be expected to maintain a relatively constant pH in the bulk solution, this may not be the case for an equivalent phosphate buffer with low-buffer capacity. The equivalent phosphate buffer is that which is predicted to match the impact that bicarbonate has on buffering the pH in the diffusion layer and at the dissolving drug surface. As bicarbonate is a comparatively ineffective buffer in the diffusion layer, the predicted matching phosphate buffer will also be ineffective compared to phosphate buffer concentrations that are commonly used for dissolution testing. However, the low-buffer capacity of phosphate will be observed in both the diffusion layer and the bulk solution. This problem could be overcome by maintaining a relatively constant bulk pH through titration. Another consideration that must be taken into account is that, as a drug particle is dissolving, the diffusion layer thickness of the particle may be considered to change.[36–38] The bicarbonate buffer model and the data for flux of ibuprofen at different rotational speeds (different diffusion layer thickness) in Krieg et al.[17] shows that the predicted pH at the surface of the drug is dependent on the diffusion layer thickness. This aspect makes the selection of an appropriate diffusion layer thickness a significant parameter for particle dissolution in bicarbonate buffer. Of course, the dosage form and excipients could affect disintegration and dissolution. This could have a significant impact on the phosphate buffer concentration that best simulates physiologically relevant bicarbonate buffer.

CONCLUSIONS

The experimental data obtained from rotating disk dissolution shows that the simultaneous diffusion and chemical reaction model accurately predicts drug flux where "instantaneous" chemical reactions occur as is the case for phosphate buffer. In the case of bicarbonate buffer, the predicted flux and experimental results show the importance of reaction kinetics in buffering the pH in the diffusion layer and at the surface of the dissolving drug. The dissolution results for the weak acids ibuprofen, indomethacin, 2-naphthoic acid, ketoprofen, benzoic acid, and the weak base haloperidol demonstrate that the experimental flux in bicarbonate buffer cannot be predicted accurately by assuming that chemical equilibrium is instantly achieved. Therefore, the reaction rates must be taken into account. Because of the slow reaction rate between CO_2 and H_2O, the BCE model overestimates and the CAI model underestimates the impact of bicarbonate buffer throughout the convective-diffusion layer and at the surface of the tablet. We show that the slow hydration and dehydration reactions can be accounted for by assuming that CO_2 does not react with H_2O in the convective-diffusion layer, whereas H_2CO_3 undergoes an irreversible chemical reaction forming CO_2 and H_2O in the convective-diffusion layer. This unique attribute of the bicarbonate buffer-diffusion-reaction system can accurately predict drug dissolution in bicarbonate buffer.

Matching the dissolution rate (flux) of weak acid and weak base drugs in phosphate and bicarbonate buffer systems is possible, but it is a complex function of buffer pH and pK_a, drug pK_a and solubility, and diffusion layer thickness. The accuracy of the IRR model to predict rotating disk dissolution in bicarbonate buffer allowed for predictions of equivalent phosphate buffer concentrations that matched physiologically relevant bicarbonate buffer for both weak acid and weak base drugs. An important conclusion of this work is that, although it is possible to identify an equivalent phosphate buffer for a drug, a precise match for dosage form testing is challenging because of the complex nature mentioned here. However, this paper provides a simple way to identify phosphate buffer concentrations that may provide a better dissolution media to simulate the dissolution of weak acid and weak base drugs *in vivo*. If the intrinsic solubility of the drug and the drug pK_a are known, Figure 8 provides a useful guide to develop a dissolution protocol using phosphate buffer concentrations that may be more *in vivo* relevant.

It appears that low phosphate buffer concentrations (1–25 mM) are often more physiologically relevant and may better simulate the impact of bicarbonate buffer on the dissolution of weak acid drugs. For weak base drugs, extremely low phosphate buffer concentrations (<2 mM) would be needed to match physiologically relevant bicarbonate buffer. These predicted equivalent phosphate buffer concentrations suggest that the current phosphate buffer concentrations used for dissolution testing (often 50 mM) likely do not accurately reflect the dissolution media and conditions that a drug will experience in the intestine.

ACKNOWLEDGMENTS

Financial support provided by USP Fellowship (2010–2012), the Chingju Wang Sheu Graduate Student Fellowship (2009–2011) AstraZeneca Grant, and FDA Contract HHSF223201310144C is gratefully acknowledged.

REFERENCES

1. FDA. 2000. Guidance for industry. Waiver of the in vivo bioavailability and bioequivalence studies for immediate-release solid oral dosage

forms based on a biopharmaceutics classification system. Washington, District of Columbia: U.S. Department of Health and Human, Food and Drug Administration (FDA), Center for Drug Evaluation and Research.
2. Aunins JG, Southard MZ, Myers RA, Himmelstein KJ, Stella VJ. 1985. Dissolution of carboxylic acids III. The effect of polyionizable buffers. J Pharm Sci 74(12):1305–1316.
3. McNamara DP, Amidon GL. 1988. Reaction plane approach for estimating the effects of buffers on the dissolution rate of acidic drugs. J Pharm Sci 77(6):511–517.
4. Sheng JJ, McNamara DP, Amidon GL. 2009. Toward an in vivo dissolution methodology: A comparison of phosphate and bicarbonate buffers. Mol Pharm 6(1):29–39.
5. USP. 2000. The United States Pharmacopeia USP 24, The National Formulary NF19. Rockville, Maryland: United States Pharmacopeial Convention.
6. Galia E, Nicolaides E, Horter D, Lobenberg R, Dressman JB. 1998. Evaluation of various dissolution media for predicting in vivo performance of class I and II drugs. Pharm Res 15(5):698.
7. McGee LC, Hastings AB. 1942. The carbon dioxide tension and acid-base balance of jejunal secretions in man. J Biol Chem 142:893–904.
8. Persson EM, Gustafsson A-S, Carlsson AS, Nilsson RG, Knutson L, Forsell P, Hanisch G, Lennernäs H, Abrahamsson B. 2005. The effects of food on the dissolution of poorly soluble drugs in human and in model small intestinal fluids. Pharm Res 22(12):2141–2151.
9. Perez de la Cruz Moreno M, Oth M, Deferme S, Lammert F, Tack J, Dressman J, Augustijns P. 2006. Characterization of fasted-state human intestinal fluids collected from duodenum and jejunum. J Pharm Pharmacol 58(8):1079–1089.
10. Kalantzi L, Goumas K, Kalioras V, Abrahamsson B, Dressman JB, Reppas C. 2006. Characterization of the human upper gastrointestinal contents under conditions simulating bioavailability/bioequivalence studies. Pharm Res 23(1):165–176.
11. Bergstrom C, Holm R, Jorgensen SA, Andersson SBE, Artursson P, Beato S, Borde A, Box K, Brewster M, Dressman J, Feng K-I, Halbert G, Kostewicz E, McAllister M, Muenster U, Thinnes J, Taylor R, Mullertz A. 2014. Early pharmaceutical profiling to predict oral drug absorption: Current status and unmet needs. Eur J Pharm Sci 57:173–199.
12. Fuchs A, Dressman JB. 2014. Composition and physicochemical properties of fasted-state human duodenal and jejunal fluid: A critical evaluation of the available data. J Pharm Sci 103:3398–3411.
13. McNamara DP, Whitney KM, Goss SL. 2003. Use of a physiologic bicarbonate buffer system for dissolution characterization of ionizable drugs. Pharm Res 20(10):1641–1646.
14. Boni JE, Brickl RS, Dressman J. 2007. Is bicarbonate buffer suitable as a dissolution medium? J Pharm Pharmacol 59(10):1375–1382.
15. Fadda HM, Merchant HA, Arafat BT, Basit AW. 2009. Physiological bicarbonate buffers: Stabilisation and use as dissolution media for modified release systems. Int J Pharm 382(1–2):56–60.
16. Liu F, Merchant HA, Kulkarni RP, Alkademi M, Basit AW. 2011. Evolution of a physiological pH 6.8 bicarbonate buffer system: Application to the dissolution testing of enteric coated products. Eur J Pharm Biopharm 78:151–157.
17. Krieg BJ, Taghavi SM, Amidon GL, Amidon GE. 2014. In vivo predictive dissolution: Transport analysis of the CO_2, bicarbonate in vivo buffer system. J Pharm Sci 103(11):3473–3490.
18. Karl AL, Majella EL, Corrigan OI. 2003. Effect of buffer media composition on the solubility and effective permeability coefficient of ibuprofen. International journal of pharmaceutics 253(1–2):49–59 [PubMed]
19. Mooney K, Mintun M, Himmelstein K, Stella V. 1981. Dissolution kinetics of carboxylic acids II: Effect of buffers. J Pharm Sci 70(1):22–32.
20. Vinograd JR, McBain JW. 1941. Diffusion of electrolytes. J Am Chem Soc 63(7):2008–2015.
21. French DL, Himmelstein KJ, Mauger JW. 1995. Physicochemical aspects of controlled release of substituted benzoic and naphthoic acids using Carbopol gel Journal of Controlled Release 37:281–289 [PubMed]
22. McMurry, J. 2010. Organic Chemistry with Biological Applications. 2nd. Belmont: Brooks/Cole.
23. Fagerberg JH, Tsinman O, Sun N, Tsinman k, Avdeef A, Bergström CAS. 2010. Dissolution rate and apparent solubility of poorly soluble drugs in biorelevant dissolution media. Molecular pharmaceutics 7(5):1419–30 [PubMed]
24. Tsinman K, Avdeef A, Tsinman O, Voloboy D. 2009. Powder dissolution method for estimating rotating disk intrinsic dissolution rates of low solubility drugs. Pharm Res 26(9):2093–2100.
25. Avdeef A, Tsinman O. 2008. Miniaturized rotating disk intrinsic dissolution rate measurement: Effects of buffer capacity in comparisons to traditional wood's apparatus. Pharm Res 25(11):2613–2627.
26. Underberg WJM, Schulman SG. 1979. Fluorimetric Determination of Acidity Constants of Naphthoic and Anthroic Acids Analytical Chimica Acta 105:311–317 [PubMed]
27. Zeebe RE. 2011. On the molecular diffusion coefficients of dissolved CO_2, HCO_3^-, and CO_3^{2-} and their dependence on isotopic mass. Geochimica et Cosmochimica Acta 75:2483–2498.
28. Garg LC, Maren TH. 1972. The rates of hydration of carbon dioxide and dehydration of carbonic acid at 37 degrees. Clinica chimica acta; international journal of clinical chemistry 261(1):70–6 [PubMed]
29. Frank MJW, Kuipers JAM, van Swaaij WPM. 1996. Diffusion Coefficients and Viscosities of $CO_2 + H_2O$, $CO_2 + CH_3OH$, $NH_3 + H_2O$, and $NH_3 + CH_3OH$ Liquid Mixtures. J Chem Eng Data 41:297–302.
30. Wilke CR, Chang P. 1955. Correlation of Diffusion Coefficients in Dilute Solutions. AlChE Journal 1:264–270.
31. Li S, Wong S, Sethia S, Almoazen H, Joshi YM, Serajuddin ATM. 2005. Investigation of solubility and dissolution of a free base and two different salt forms as a function of pH. Pharm Res 22(4):628–635.
32. Li S, Doyle P, Metz S, Royce AE, Serajuddin AT. 2005. Effect of chloride ion on dissolution of different salt forms of haloperidol, a model basic drug. J Pharm Sci 94(10):2224–2231.
33. Fagerberg J, Al-Tikriti Y, Ragnarsson G, Bergstrom C. 2012. Ethanol effects on apparent solubility of poorly soluble drugs in simulated intestinal fluid. Mol Pharm 9:1942–1952.
34. Garbacz G, Kolodziej B, Koziolek M, Weitschies W, Klein S. 2014. A dynamic system for the simulation of the fasting luminal pH-gradients using hydrogen carbonate buffers for dissolution testing of ionisable compounds. Eur J Pharm Sci 51:224–231.
35. Mudie DM, Amidon GL, Amidon GE. 2010. Physiological parameters for oral delivery and in vitro testing. Mol Pharm 7(5):1388–1405.
36. Hintz RJ, Johnson KC. 1989. The effect of particle size distribution on dissolution rate and oral absorption. Int J Pharm 51:9–17.
37. Wang J, Flanagan DR. 1999. General solution for diffusion-controlled dissolution of spherical particles 1. Theory. J Pharm Sci 88(7):731–738.
38. Sheng JJ, Sirois PJ, Dressman JB, Amidon GL. 2008. Particle diffusional layer thickness in a USP dissolution apparatus II: A combined function of particle size and paddle speed. J Pharm Sci 97(11):4815–4829.